Physics Letters B 701 (2011) 562–567

Contents lists available at ScienceDirect

Physics Letters B

www.elsevier.com/locate/physletb

Determination of the η-transition form factor in the $\gamma p \to p\eta \to p\gamma e^+e^-$ reaction

H. Berghäuser [a,*,1], V. Metag [a], A. Starostin [b], P. Aguar Bartolomé [c], L.K. Akasoy [c], J.R.M. Annand [d], H.J. Arends [c], K. Bantawa [e], R. Beck [f,c], V. Bekrenev [g], A. Braghieri [h], D. Branford [i], W.J. Briscoe [j], J. Brudvik [b], S. Cherepnya [j], B.T. Demissie [j], E.J. Downie [c], P. Drexler [a], M. Dieterle [k], L.V. Fil'kov [g], A. Fix [l], D.I. Glazier [i], E. Heid [c], D. Hornidge [m], O. Jahn [c], T.C. Jude [g], V.L. Kashevarov [c,g], A. Knezevic [n], R. Kondratiev [o], M. Korolija [n], M. Kotulla [a], A. Koulbardis [p], S. Kruglov [p], B. Krusche [k], B. Lemmer [a], V. Lisin [o], K. Livingston [d], I.J.D. MacGregor [d], Y. Maghrbi [k], D.M. Manley [e], M. Martinez-Fabregate [c], J.C. McGeorge [d], E.F. McNicoll [d], D. Mekterovic [n], S. Micanovic [n], A. Mushkarenkov [h], B.M.K. Nefkens [b], A. Nikolaev [f], R. Novotny [a], M. Ostrick [c], R.O. Owens [d], P. Pedroni [h], F. Pheron [k], A. Polonski [o], J. Robinson [d], S.N. Prakhov [b], G. Rosner [d], T. Rostomyan [k], S. Schumann [c], D. Sober [q], I.M. Suarez [b], I. Supek [n], C.M. Tarbert [i], M. Thiel [a], A. Thomas [c], M. Unverzagt [c], D.P. Watts [i], D. Werthmüller [k], I. Zamboni [n], F. Zehr [k]

[a] *II. Physikalisches Institut, Universität Giessen, Giessen, Germany*
[b] *University of California at Los Angeles, Los Angeles, CA, USA*
[c] *Institut für Kernphysik, Johannes Gutenberg-Universität Mainz, Mainz, Germany*
[d] *Department of Physics and Astronomy, University of Glasgow, Glasgow, UK*
[e] *Kent State University, Kent, OH, USA*
[f] *Helmholtz-Institut für Strahlen- und Kernphysik, Universität Bonn, Bonn, Germany*
[g] *Lebedev Physical Institute, Moscow, Russia*
[h] *INFN Sezione di Pavia, Pavia, Italy*
[i] *School of Physics, University of Edinburgh, Edinburgh, UK*
[j] *Center for Nuclear Studies, George Washington University, Washington, DC, USA*
[k] *Institut für Physik, Universität Basel, Basel, Switzerland*
[l] *Tomsk Polytechnic University, Tomsk, Russia*
[m] *Mount Allison University, Sackville, NB, Canada*
[n] *Rudjer Boskovic Institute, Zagreb, Croatia*
[o] *Institute for Nuclear Research, Moscow, Russia*
[p] *Petersburg Nuclear Physics Institute, Gatchina, Russia*
[q] *The Catholic University of America, Washington, DC, USA*

ARTICLE INFO

Article history:
Received 20 May 2011
Received in revised form 22 June 2011
Accepted 22 June 2011
Available online 28 June 2011
Editor: D.F. Geesaman

Keywords:
Meson decays
Transition form factor

ABSTRACT

The Dalitz decay $\eta \to \gamma e^+e^-$ has been measured using the combined Crystal Ball and TAPS photon detector setup at the electron accelerator MAMI-C. Compared to the most recent transition form-factor measurement in the e^+e^- channel, statistics have been improved by one order of magnitude. The e^+e^- invariant mass distribution shows a deviation from the QED prediction for a point-like particle, which can be described by a form-factor. Using the usual monopole transition form-factor parameterization, $F(m^2) = (1 - m^2/\Lambda^2)^{-1}$, a value of $\Lambda^{-2} = (1.92 \pm 0.35(stat) \pm 0.13(syst))$ GeV^{-2} has been determined. This value is in good agreement with a recent measurement of the η Dalitz decay in the $\mu^+\mu^-$ channel and with recent form-factor calculations. An improved value of the branching ratio $\mathrm{BR}(\eta \to \gamma e^+e^-) = (6.6 \pm 0.4(stat) \pm 0.4(syst)) \cdot 10^{-3}$ has been determined.

1. Introduction

Electromagnetic transition form factors are an important tool for studying the intrinsic structure of hadrons. For point-like particles the decay rates can be exactly calculated within Quantum

* Corresponding author.
E-mail address: henning.berghaeuser@exp2.physik.uni-giessen.de (H. Berghäuser).
[1] II. Physikalisches Institut, Heinrich-Buff-Ring 16, D-35392 Giessen, Germany.

0370-2693/$ – see front matter
doi:10.1016/j.physletb.2011.06.069

Electrodynamics (QED). Information on the intrinsic structure is encoded in the multiplicative transition form factor. The decay of light pseudoscalar mesons π^0, η, and η' into a real and a virtual photon are of particular interest as they allow a test of the validity of the vector meson dominance (VMD) assumption where the coupling of a photon to a hadron is mediated by a virtual vector meson. Furthermore, the transition form factor can be studied for momentum transfers not accessible in scattering or annihilation experiments. New theoretical efforts aim at a systematic description of the dynamics of light pseudoscalar and vector mesons and their coupling to electromagnetism [1]. Here electromagnetic transition form factors of vector mesons [2] and pseudoscalar mesons [3] provide an excellent tool to test the predictions of the leading-order calculations and to stimulate calculations beyond leading order. These theoretical activities have demonstrated the need for improved experimental data. An overview of earlier work in the field can be found in [4].

In this work the Dalitz decay of the η meson $\eta \to \gamma\gamma* \to \gamma e^+e^-$ has been investigated. The invariant mass distribution of the dilepton pairs is given by [4]

$$\frac{d\Gamma(\eta \to l^+l^-\gamma)}{dm\,\Gamma(\eta \to \gamma\gamma)} = \frac{4\alpha}{3\pi m}\cdot\left[1-\frac{4m_l^2}{m^2}\right]^{\frac{1}{2}}\cdot\left[1+2\frac{m_l^2}{m^2}\right]\cdot\left[1-\frac{m^2}{m_\eta^2}\right]^3\cdot\left|F_\eta(m^2)\right|^2 = [\mathrm{QED}]\cdot\left|F_\eta(m^2)\right|^2. \quad (1)$$

Here, l stands for either e or μ, depending on the decay channel chosen; m corresponds to the mass of the dilepton pair and m_η to the mass of the η meson, respectively. In the vector meson dominance assumption the form factor is usually parametrized by

$$F(m^2) = \frac{1}{1-\frac{m^2}{\Lambda^2}}. \quad (2)$$

The only parameter in this one-pole approximation is the slope b of the form factor for $m^2 = 0$, which is related to the effective virtual vector meson mass Λ by

$$b = \left.\frac{dF}{dm^2}\right|_{m^2=0} = \Lambda^{-2}. \quad (3)$$

Measurements of this form factor have been reported by the SND Collaboration [5] in the $\eta \to \gamma e^+e^-$ channel and by the Lepton-G experiment [6] in the $\eta \to \gamma\mu^+\mu^-$ decay mode. More recently a precision measurement was performed by the NA60 Collaboration [7] in the $\mu^+\mu^-$ channel, but without detecting the photon and thus without reconstructing the η meson from its decay products. With a value of $\Lambda^{-2} = (1.6 \pm 2.0)$ GeV^{-2} the accuracy of the SND experiment was insufficient to establish a deviation from the QED prediction, which was the main motivation to repeat this measurement in the $\eta \to \gamma e^+e^-$ channel under improved conditions.

2. Experiment

The experiment was performed at the electron accelerator MAMI-C in Mainz using the combined Crystal Ball (CB) [8] and TAPS [9] detectors. Energy-tagged photons were produced via the bremsstrahlung process in the Glasgow–Mainz tagging facility [10,11] and impinged on a liquid hydrogen target. The quasi-monochromatic photon beam covered an energy range from 617 to 1402 MeV and had an intensity of $2 \cdot 10^5$(4 MeV)$^{-1}$ s^{-1} at 620 MeV. The bremsstrahlung photons, produced by the electrons in a 10 µm copper radiator, were collimated by a lead collimator that was 4 mm in diameter; the resulting diameter of the photon beam spot on the target was approximately 1 cm. The target itself had a diameter of 3 cm and a length of 4.76 cm and was located in the center of the Crystal Ball detector. The material budget around the target, including the Kapton cell and the 1 mm thick carbon-fiber beamline, amounted to 0.8% of a radiation length X_0, which was essential for suppressing the conversion of real photons into e^+e^- pairs.

By combining the Crystal Ball with the TAPS calorimeter in a forward wall configuration, photons and charged particles were registered over the full azimuthal angular range. Polar angles of

Table 1
Applied cuts in the η-Dalitz analysis of simulated and real-data events.

Cut-Nr.	Name [Unit]	Limits
1	Momentum balance X vs. energy balance	2D-Cut see Fig. 3
2	Momentum balance Y vs. energy balance	2D-Cut
3	Momentum balance Z [MeV]	−100.0–105.0
4	Missing mass [MeV]	900–960
5	Beam energy [MeV]	750–1210
6	Coplanarity [°]	167–193
7	Θ_{proton} [°]	0–50
8	Opening angle e^+e^- [°]	10–140
9	$e^\pm$ cluster size	4–14
10	Angle $e^\pm\gamma$ [°]	50–175

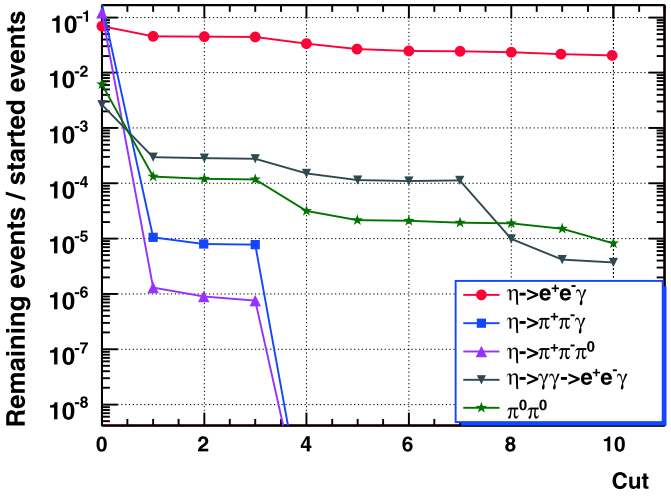

Fig. 1. The reduction of background events and the acceptance for the $\gamma p \to p\gamma e^+e^-$ channel for the cuts listed in Table 1.

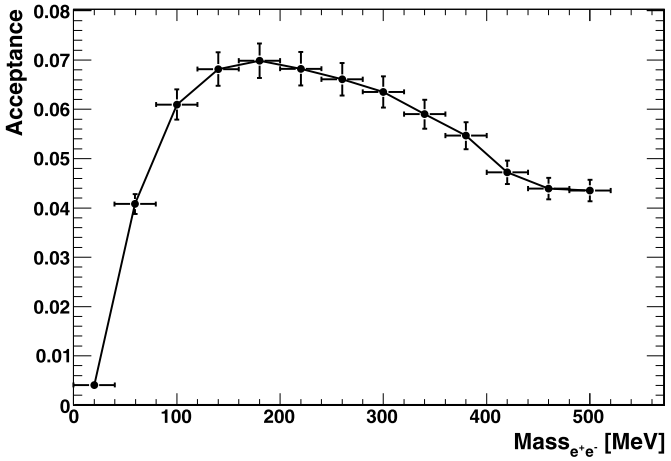

Fig. 2. Acceptance for the $\gamma p \to p\eta \to p\gamma e^+e^-$ reaction as a function of the e^+e^- invariant mass simulated with the PLUTO event generator [15] and the GEANT 4 code.

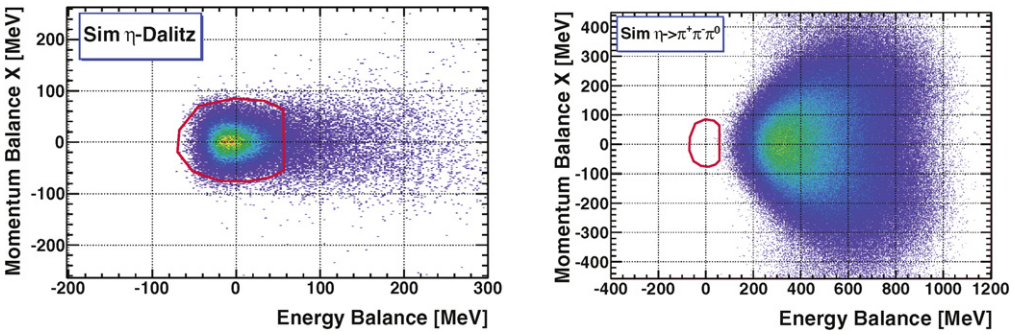

Fig. 3. Simulation of the energy-momentum balance for the $\gamma p \to p\eta \to p\gamma e^+e^-$ reaction (left) and for the $\gamma p \to p\eta \to p\pi^+\pi^-\pi^0$ reaction (right). In the latter case the charged pions are assumed to be misidentified as electrons.

1°–20° were subtended by the 384 BaF_2 scintillator modules (12 X_0) of TAPS and polar angles of 21°–160° were covered by the 672 NaI scintillator modules (15.7 X_0) of the CB. Charged particles were identified in plastic scintillators of 2 mm and 5 mm thickness mounted in front of the NaI and BaF_2 scintillator modules, respectively. A more detailed description of the detector setup has recently been given in [12].

The data were collected during two running periods totalling 350 h. In addition, about 70 hours with a beam of twice the photon beam intensity were used for a measurement with an empty target. The trigger threshold for the total energy deposited in the Crystal Ball detector was 350 MeV; furthermore a multiplicity trigger was used requiring two or more hits with energy depositions larger than 20 MeV in the TAPS or CB detectors (for details see [13]). In the data analysis clusters of at least 50 MeV are requested to suppress photon split-offs (see [14]).

3. Analysis procedure

The reconstruction of a weak channel like $\gamma p \to p\eta \to p\gamma e^+e^-$ among several strong background channels is a major experimental challenge. The identification of the final-state particles is hampered by the fact that the detector system does not provide a magnetic field for particle tracking. Only the energy and angle of the registered particles are available as well as the information whether they are charged or neutral. The sign of the charge cannot be determined. Electrons and pions can be separated from protons by the energy loss in the plastic scintillators. A rough separation between electrons and pions is achieved by requesting for electron candidates a higher multiplicity of responding detector modules within a given cluster in the calorimeters. For pions corresponding multiplicities are typically 2–3.

Only events with at least one proton, one photon and two electron candidates were selected for further processing. A rare final state like in the $\eta \to \gamma e^+e^-$ Dalitz decay can only be identified among the many background channels by exploiting the complete kinematics of the $\gamma p \to p\eta \to p\gamma e^+e^-$ reaction in an exclusive analysis. Several cuts were applied to select the reaction of interest in the sequence given in Table 1.

The same cuts were applied to Monte Carlo simulations of possible background reactions. Typically 2–10 million events were simulated for the background channels, assuming phase space distributions, and 5 million events for the $\gamma p \to p\eta \to p\gamma e^+e^-$ reaction. For the latter the PLUTO event generator [15] was used. All together 67 cut settings were investigated in order to find a compromise between statistics in the channel of interest and background suppression. The rejection power of each cut and the remaining acceptance for the η Dalitz decay are shown in Fig. 1 for the cut setting finally chosen. The dependence of the

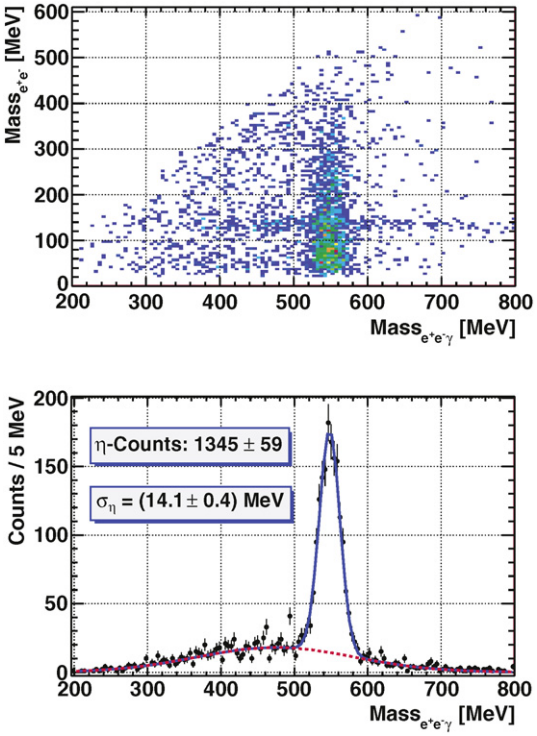

Fig. 4. Distribution of reconstructed $e^+e^-\gamma$ candidate events after applying the cuts given in Table 1. The lower figure shows the projection onto the $e^+e^-\gamma$ mass axis.

$p\gamma e^+e^-$ acceptance on the $\text{Mass}_{e^+e^-}$ is shown in Fig. 2. The fall off towards small invariant masses arises from cuts on the cluster energies and opening angles and introduces systematic uncertainties estimated to be 5%. The mass-averaged acceptance is (2.0 ± 0.1)%.

Pions misidentified as electrons were rejected by cuts on the energy and momentum balance calculated from the entrance channel and all registered final-state particles (cuts 1, 2) as demonstrated by simulations shown in Fig. 3. An additional cut on the nucleon missing mass led to a suppression of $\pi^+\pi^-$ pairs relative to e^+e^- pairs of $1 \cdot 10^{-7}$. $\eta \to 2\gamma$ decays with a subsequent conversion of one photon in the target or surrounding material were particularly suppressed by a cut on the opening angle of the e^+e^- pair, as one would expect for real photon conversion (cut 8).

The events surviving all cuts listed in Table 1 are shown in Fig. 4 where the invariant e^+e^- mass is plotted versus the γe^+e^- mass. On top of a smooth background distribution, the projection onto the x-axis exhibits a peak at the η mass with

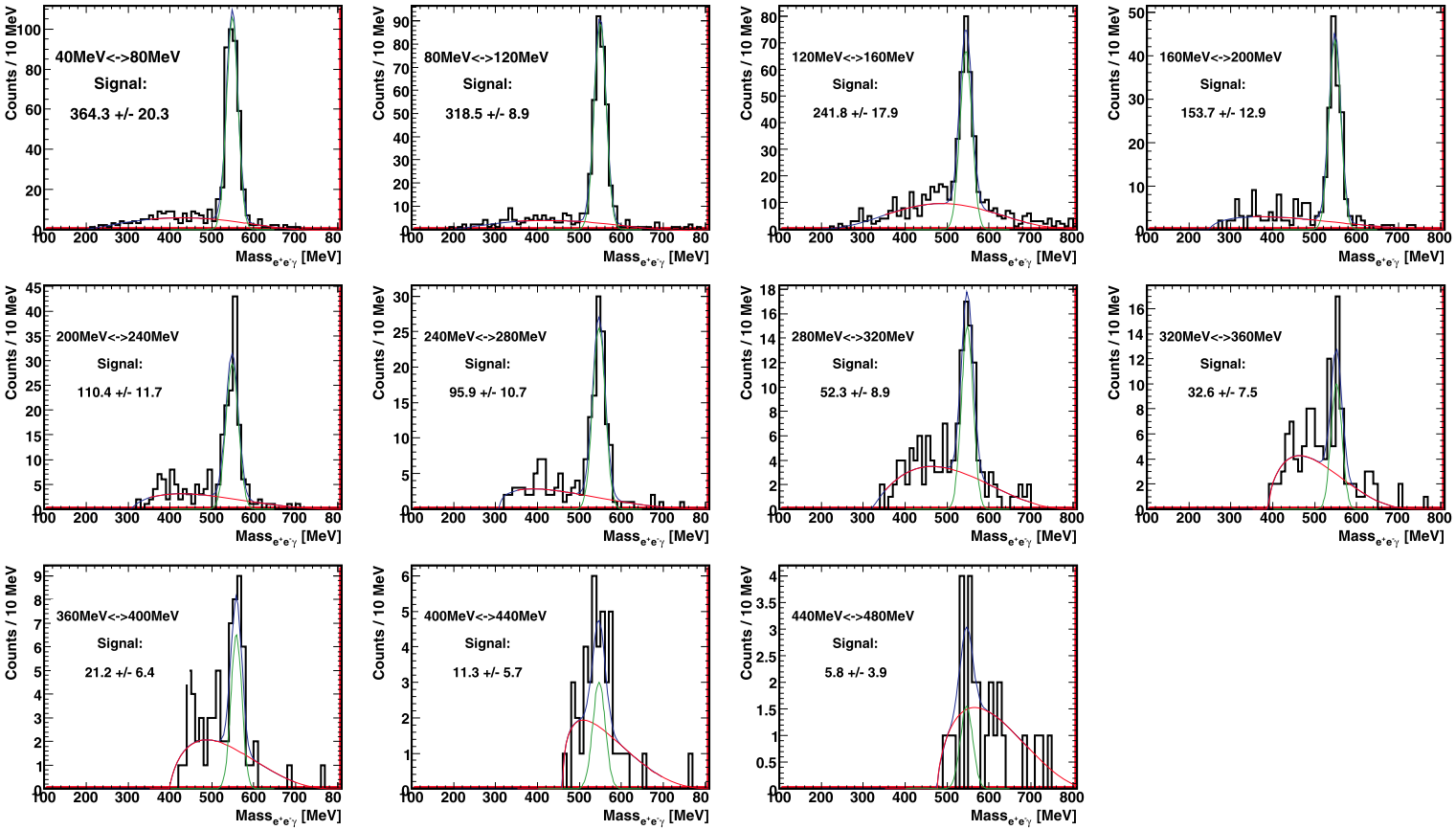

Fig. 5. Fits to γe^+e^- invariant mass distributions for different Mass$_{e^+e^-}$ bins.

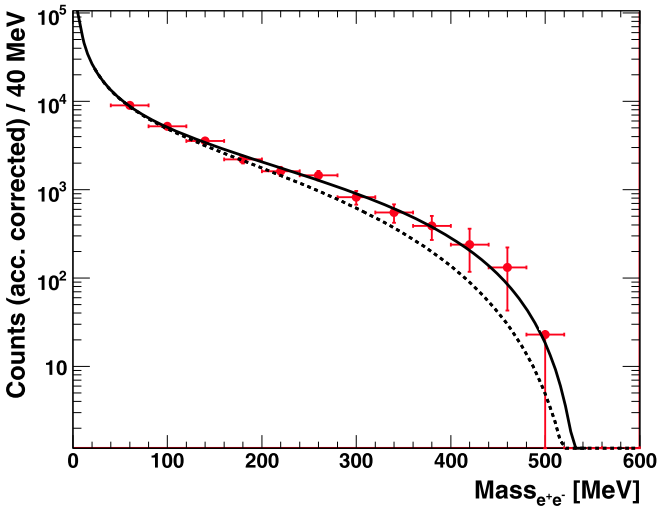

Fig. 6. Invariant e^+e^- mass distribution of reconstructed events after acceptance correction. The errors given are purely statistical. The solid curve is a fit within the VMD-model using a monopole form factor (Eq. (1)). The dotted curve is the QED prediction.

1345 ± 59 counts and a resolution of $\sigma = 14.1 \pm 0.4$ MeV consistent with simulations. A band near the π^0 mass of 135 MeV seen in the two-dimensional plot corresponds to $2\pi^0$ production events where two photons from a $\pi^0 \to \gamma\gamma$ decay were misidentified as electrons and one photon is not detected. The intensity of $\eta \to \gamma\gamma* \to \gamma e^+e^-$ events as a function of the e^+e^- invariant mass $\text{Mass}_{e^+e^-}$ was determined by fitting the γe^+e^- mass distributions for different slices in $\text{Mass}_{e^+e^-}$ as shown in Fig. 5. In the fits the peak position and the width were constrained to 540–560 MeV and 11–20 MeV, respectively. The fit errors increase with mass and reach a value of $\approx 50\%$ for the highest mass bins.

4. Results

Using Eq. (1) for extracting the transition form factor from the data implies the determination of the $\eta \to e^+e^-\gamma$ yield relative to the number of $\eta \to \gamma\gamma$ decays. An analysis of the latter decay mode, using the acceptance of 12.1% derived from Monte Carlo simulations for the $\gamma p \to p\eta \to p\gamma\gamma$ reaction, determined the number of $\eta \to \gamma\gamma$ decays to be $(4.01 \pm 0.18) \cdot 10^6$. Using the branching ratio $\text{BR}(\eta \to \gamma\gamma) = 39.3\%$ listed in the *Review of Particle Physics* [16] the total number of produced η mesons corresponds to $(10.2 \pm 0.45) \cdot 10^6$. With the 1345 reconstructed $\eta \to \gamma e^+e^-$ decays and the acceptance of $(2.0 \pm 0.1)\%$, a ratio of decay widths $\Gamma_{\eta\to\gamma e^+e^-}/\Gamma_{\eta\to\gamma\gamma} = (1.68 \pm 0.10) \cdot 10^{-2}$ was deduced. This corresponds to a branching ratio $\text{BR}(\eta \to \gamma e^+e^-) = (6.6 \pm 0.4(stat) \pm 0.4(syst)) \cdot 10^{-3}$ to be compared to the current PDG value of $(7.0 \pm 0.7) \cdot 10^{-3}$.

After correcting for the e^+e^- mass-dependent acceptance of the $\gamma p \to p\eta \to p\gamma e^+e^-$ reaction (see Fig. 2) the invariant e^+e^- mass distribution shown in Fig. 6 was obtained. The spectrum was fitted according to Eq. (1) with two parameters, the slope b of the form factor and a normalization constant.

Dividing the data points in Fig. 6 by the QED prediction (see Eq. (1)) the η transition form factor shown in Fig. 7 was deduced. The present data show an enormous improvement in the e^+e^- channel compared to the previous work of the SND Collaboration who reconstructed only 110 $\eta \to \gamma e^+e^-$ events. With 1345 reconstructed events the statistics could be improved by an order of magnitude. The statistics obtained by the NA60 Collaboration are clearly superior but, due to choosing the $\mu^+\mu^-$ channel, their data points only start at dilepton masses above 200 MeV. The data points in the present analysis get closer to the photon point and reach invariant mass values as low as 40 MeV. Furthermore, due to the identification of all final-state particles, the η meson could be fully reconstructed in contrast to the NA60 analysis where the photon was not detected and the form factor was deduced by unfolding the $\mu^+\mu^-$ invariant mass spectrum, which also contained contributions from other particles.

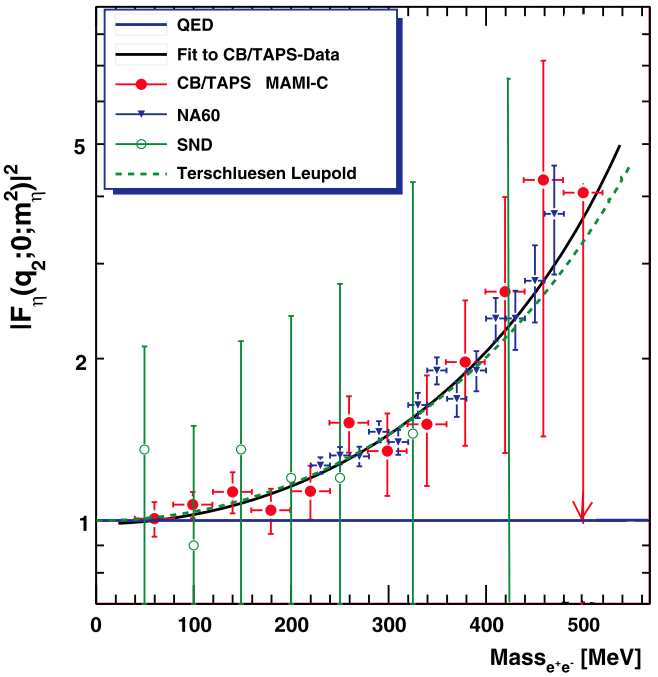

Fig. 7. η-Dalitz transition form factor: The red circles are the data of this work (the black curve is the fit to the data). The data point at $\text{Mass}_{ee} = 500$ MeV represents an upper limit. The green (open) circles show the result of the SND experiment [5]. The blue (inverted) triangles represent the result obtained by NA60 [7] in the $\mu^+\mu^-$ channel. The green (dashed) curve is a calculation performed by [3]. (For interpretation of the references to color in this figure legend, the reader is referred to the web version of this Letter.)

From the fit, the slope of the η-meson transition form factor was determined as

$$b = \left.\frac{dF}{dm^2}\right|_{m^2=0} = \Lambda^{-2} = \left(1.92 \pm 0.35(stat) \pm 0.13(syst)\right) \text{GeV}^{-2}, \quad (4)$$

corresponding to $\Lambda = (720 \pm 60(stat) \pm 25(syst))$ MeV. The systematic uncertainty was estimated from a comparison of the results obtained in the 67 different cut settings. The fit results were remarkably stable for the individual cut settings. The systematic error was taken as the *rms* deviation of the individual values from the average. The ratio of systematic to statistical errors was 0.4 for the pole mass and 1.0 for the branching ratio, respectively. The fit parameters are more precise than the earlier SND result in the e^+e^- channel of $\Lambda^{-2} = (1.6 \pm 2.0)$ GeV^{-2} [5] and are consistent with the values reported in the $\mu^+\mu^-$ channel by Lepton-G: $\Lambda^{-2} = (1.9 \pm 0.4)$ GeV^{-2} [6] and by NA60: $\Lambda^{-2} = (1.95 \pm 0.17(stat) \pm 0.05(syst))$ GeV^{-2} [7]. The value for the Λ parameter is in excellent agreement with the predictions of the VMD model of $\Lambda = 730$–750 MeV, depending on the η–η' mixing angle [4,17]. The fit to the present data is very close to the calculation by Terschlüsen and Leupold [2,3] who studied form factors

in the decays of light mesons in a recently proposed scheme that treats pseudoscalar and vector mesons as active degrees of freedom [1]. This work calls for further improved experimental data.

5. Conclusion and outlook

In this work the transition form factor of the η-Dalitz decay was measured in the $\eta \to e^+e^-\gamma$ channel with statistics improved by an order of magnitude compared to the most recent form-factor measurement in this channel [5]. The result is in good agreement with previous measurements from [6,7] and with most recent theoretical calculations [2,3]. After establishing that weak channels like the η Dalitz decay can be identified in an exclusive analysis using a 4π calorimeter without magnetic field, this experimental approach can be extended to the measurement of form factors of other pseudoscalar and vector mesons.

Acknowledgements

The authors wish to acknowledge the excellent support of the accelerator group and operators of MAMI. We appreciate illuminating discussions with Carla Terschlüsen and Stefan Leupold on their calculations. This work was supported by the Deutsche Forschungsgemeinschaft (SFB 443, SFB/TR16), DFG-RFBR (Grant No. 09-02-91330), the European Community-Research Infrastructure Activity under the FP6 "Structuring the European Research Area" programme (Hadron Physics, contract number RII3-CT-2004-506078), Schweizerischer Nationalfonds, the UK EPSRC and STFC, US DOE, US NSF, and NSERC (Canada). We thank the undergraduate students of Mount Allison and The George Washington Universities for their assistance.

References

[1] M.F.M. Lutz, S. Leupold, Nucl. Phys. A 813 (2008) 96.
[2] C. Terschlüsen, S. Leupold, Phys. Lett. B 691 (2010) 191.
[3] C. Terschlüsen, Diploma Thesis, Univ. of Giessen, 2010, http://www.uni-giessen.de/cms/fbz/fb07/fachgebiete/physik/einrichtungen/theorie/theorie1/publications/diploma.
[4] L.G. Landsberg, Phys. Rep. 128 (1985) 301.
[5] M.N. Achasov, et al., Phys. Lett. B 504 (2001) 275.
[6] R.I. Djhelyadin, et al., Phys. Lett. B 94 (1980) 548.
[7] R. Arnaldi, et al., Phys. Lett. B 677 (2009) 260.
[8] A. Starostin, et al., Phys. Rev. C 64 (2001) 055205.
[9] R. Novotny, IEEE Trans. Nucl. Sci. 38 (1991) 379;
A.R. Gabler, et al., Nucl. Instr. Meth. A 346 (1994) 168.
[10] I. Anthony, J.D. Kelly, S.J. Hall, G.J. Miller, Nucl. Instr. Meth. A 301 (1991) 230.
[11] S.J. Hall, G.J. Miller, R. Beck, P. Jennewein, Nucl. Instr. Meth. 368 (1996) 698.
[12] V.L. Kashevarov, et al., Eur. Phys. J. A 42 (2009) 141.
[13] M. Unverzagt, et al., Eur. Phys. J. A 39 (2009) 169.
[14] M. Nanova, et al., Phys. Rev. C 82 (2010) 035209.
[15] I. Fröhlich, et al., PoS ACAT2007 (2007) 076, arXiv:0708.2382 [nucl-ex].
[16] K. Nakamura, et al., Particle Data Group, J. Phys. G 37 (2010) 075021.
[17] S. Leupold, Univ. of Uppsala, private communication, 2011.